Supplemental materials

Carnitine O-octanoyltransferase is a novel contributing factor in vascular calcification via promoting fatty acid metabolism and mitochondrial dysfunction

Takehito Okui[1,†], Masaya Iwashita[1,†], Maximillian A. Rogers[1,†], Arda Halu[1], Samantha K. Atkins[1], Shiori Kuraoka[1], Ilyes Abdelhamid[1], Hideyuki Higashi[1], Ashisha Ramsaroop[1], Masanori Aikawa[1,2], Sasha A. Singh[1], Elena Aikawa[1,2,3,*].

[1]Center for Interdisciplinary Cardiovascular Sciences, Division of Cardiovascular Medicine, Brigham and Women's Hospital, Harvard Medical School, Boston, MA, 02115, USA
[2]Center for Excellence in Vascular Biology, Cardiovascular Division, Brigham and Women's Hospital, Harvard Medical School, Boston, MA, 02115, USA
[3]Department of Human Pathology, Sechenov First Moscow State Medical University, Moscow, 119992, Russia

[†]These authors contributed equally

Running title:
CROT is a novel contributing factor to vascular calcification

[*]**Corresponding author:**
Elena Aikawa, MD, PhD
Brigham and Women's Hospital, Harvard Medical School,
3 Blackfan Street, 17th Floor, Boston, MA 02115,
Phone: 617-730-7755, Fax: 617-730-7791
eaikawa@bwh.harvard.edu

Keywords: CROT, cardiovascular calcification, smooth muscle cells, mitochondria, EPA, proteomics, lipidomics

Subject codes: Cell Signaling/Signal Transduction, Vascular Disease

Total number of supplemental figures: 9

Total number of supplemental tables: 2

TOC category and TOC subcategory: Translational and Vascular Biology

Supplemental methods

Immunohistochemistry

Human carotid artery samples were obtained from patients undergoing endarterectomy (Brigham and Women's Hospital Institutional Review Board protocol #1999P001348, the IRB approved a waiver of informed consent and authorization for the use of excess human material from clinical procedures that would otherwise be discarded, in compliance with federal regulation 45 CFR 46.116., the demographic and clinical information of donors is not available). Human carotid artery sections were embedded in Premium Frozen Section Compound (VWR International, LLC., Cat#: 95057-838) and snap-frozen. 4 μm fresh frozen sections were made using a cryostat (Leica Biosystems) and fixed with 4% paraformaldehyde for 5 minutes. After rinsing with water twice and washing twice with PBS for 5 minutes, sections were incubated with 0.3% hydrogen peroxide for 3 minutes. Sections were rinsed with water and then with PBS for 5 minutes. Sections were then covered with 4% normal serum for 30 minutes for blocking. After tapping off blocking serum, primary antibody solution was put on the sections (antibody dilutions included in Supplementary Major Resourse Table) and incubated for 1 hour. Sections were washed twice with PBS for 5 minutes and incubated with secondary antibody solution for 30 minutes. After washing twice with PBS for 5 minutes, sections were treated with ABC solution (VECTASTAIN® Elite® ABC HRP Kit, Vector Laboratories, Cat#: PK-6100) for 30 minutes. Sections were then washed twice with PBS for 5 minutes and incubated with DAB solution prepared from DAB 50× Concentrate, Brown, Horseradish Peroxidase Substrate (MilliporeSigma, Cat#: ES005-10ML). After rinsing twice with water for 5 minutes, counterstaining was performed using MilliporeSigma™ Hematoxylin solution (Gill III) (Fisher Scientific, Cat#: M1051740500).

Immunofluorescence

Human carotid artery sections were prepared and fixed using same method as with tissue immunohistochemistry. After rinsing twice with water and washing twice with PBS for 5 minutes, sections were incubated with 4% normal serum for 30 minutes for blocking. After tapping off blocking serum, primary antibody solution was put on the sections (antibody concentrations included in Supplementary Major Resources Table) and incubated for 1 hour. Sections were washed twice with PBS for 5 minutes and incubated with secondary antibody solution for 30 minutes. After washing sections twice with PBS for 5 minutes, sections were then incubated with DAPI (4',6-Diamidino-2-Phenylindole, Dihydrochloride) (Thermo Fisher Scientific Inc., Cat#: D1306) for nuclear counterstaining. Sections were imaged using confocal microscopy on a Nikon confocal A1 scope (Nikon Corporation).

Quantitative real-time PCR

RNA of human coronary artery smooth muscle cells (SMCs) was collected using TRIzol® reagent (Thermo Fisher Scientific Inc., Cat#: 15596-018) at days 0, 0.5, 1, 3, 7, 14 and 21 after switching from NM to OM (or NM for controls). Total RNA was extracted using the manufacturer's protocol. 1 μg of total RNA from each sample was reverse transcribed using qScript cDNA Synthesis Kit (Quantabio, Cat#: 95047) according to manufacturer's protocol. PCR reactions were performed using PerfeCTa® qPCR FastMix® II, ROX™ (Quantabio, Cat#: 95119), TaqMan gene expression assays primers listed in

Supplementary Major Resources table. Real time PCR was performed on a 7900HT Fast Real-Time PCR system (Thermo Fisher Scientific Inc.). The relative value of mRNA abundance was calculated using a standard curve that was made through measuring the dilution series of mixed samples.

TNAP activity assay

SMCs incubated with siRNA and OM in 24-well plates were collected 14 days after switching from NM to OM (or NM for controls). Cells protein lysates were harvested using 120 µL/well of ALP Assay Buffer (Alkaline Phosphatase Activity Colorimetric Assay Kit, BioVision Inc., Cat#: K412). Lysate samples were sonicated and centrifuged at 10,000 times gravity for 10 minutes, and supernatants were collected. TNAP activity was measured using Alkaline Phosphatase Activity Colorimetric Assay Kit according to manufacturer'sprotocol. TNAP activity was normalized to abundance of total protein measured using Pierce™ BCA Protein Assay Kit (Thermo Fisher Scientific Inc., Cat#: 23225).

Alizarin red stain

SMCs treated with siRNA and OM in 24-well plates were stained with Alizarin red staining at days 21 after switching from NM to OM (or NM for controls). Briefly, cells were washed with PBS twice, fixed with 4% formaldehyde for 10 minutes, then stained with 2% Alizarin Red Stain (Lifeline Cell Technology, Cat#: CM-0058) for 15 minutes. After washing with water three times, pictures were taken. For CROT overexpression studies, SMCs were incubated with adenovirus vectors and OM in 24-well plates and Alizarin red stain was performed 14 days after switching from NM to OM (or NM for controls).

Calcification and collagen fluorescence staining

Calcification fluorescence staining was performed through incubating cells with OsteoSense 680EX (PerkinElmer Life & Analytical Sciences, Inc. Cat#: NEV10020EX) overnight at 37°C (1:100). Collagen was stained with the CNA collagen probe (provided by Carlijn Bouten) through incubating cells at 37°C with CNA probe (1:50) for 1 hour prior to fixation.

Cell proliferation assay

SMCs were treated with siRNA and OM in 96-well plates, and the assay was performed by using CyQUANT Cell Proliferation Assay Kit (Thermo Fisher Scientific, Cat#: C7026) at days 7 after switching from NM to OM (or NM for controls).

Pro-collagen 1A1 ELISA

Day 5-7 culture media of SMCs treated with siRNA and OM was collected, and ELISA was performed by using Human Pro-Collagen I alpha 1 DuoSet ELISA (R&D Systems, Inc. Cat#: DY6220-05).

CROT and H327A-CROT overexpression

EZShuttle™ Gateway® PLUS ORF Clone with human CROT (GeneCopoeia, Inc., Cat#: GC-A3413-CF) was purchased, and PCR was performed (see Supplemental Major Resourses Table for primer list) using PrimeSTAR® Max DNA Polymerase (Takara Bio Inc., Cat#: R045A) to obtain EZShuttle™ Gateway® PLUS ORF Clone with human

H327A-CROT plasmid. After treating PCR product with DpnI restriction enzyme (New England Biolabs., Cat#: R0176S), transformation was performed using One Shot™ MAX Efficiency™ DH5α-T1R Competent Cells (Thermo Fisher Scientific Inc., Cat#: 12297016). EZShuttle™ Gateway® PLUS ORF Clone with human CROT or H327A-CROT plasmid was increased by incubating transformed *E.coli* and purified using EndoFree Plasmid Maxi Kit (10) (QIAGEN, Cat#: 12362). Plasmid vectors for adenovirus expression were made through LR reaction using pAd/CMV/V5-DEST™ (Thermo Fisher Scientific Inc., Cat#: V49320) and Gateway® LR Clonase® II Enzyme Mix (Thermo Fisher Scientific Inc., Cat#: 11791-020) according to manufacturer's protocol, producing pAd/CMV/CROT/V5 and pAd/CMV/H327A-CROT/V5. Sequence of each plasmid was confirmed by sequencing analysis (Eton Bioscience, Inc.). After treating plasmids with PacI restriction enzyme (New England Biolabs., Cat#: R0547S) and purifying single-stranded DNA using QIAEX II Gel Extraction Kit (150) (QIAGEN, Cat#: 20021), DNA was transfected into HEK293A cells (Thermo Fisher Scientific Inc., Cat#: R70507) using Lipofectamine™ 2000 Transfection Reagent (Thermo Fisher Scientific Inc., Cat#: 11668019) according to manufacturer's protocol. pAd/CMV/V5-GW/lacZ (Thermo Fisher Scientific Inc., Cat#: V49320) was used as a control. Adenoviral vectors were collected from culture medium and cells through repeating freeze-thawing cycles. Multiplicity of infection (MOI) of adenoviral vectors was measured using Adeno-X™ Rapid Titer Kit (Takara Bio Inc., Cat#: 632250). SMCs were seeded at day -3 (3 days before media exchange) with 1.0×10^5 cells/mL using smooth muscle cell growth medium 2 in 24-well plates (0.5 mL/well). Smooth muscle cell growth medium 2 was replaced with NM and the first transduction using adenoviral vectors was performed the next day (day -2). At Day 0 media was exchanged from NM into OM (or NM for controls). After day 0, media exchange was performed every 3-4 days and transduction using adenoviral vectors was performed every 7 days at 200 MOI.

SMCs tandem mass tagging proteomics

SMCs were harvested using RIPA lysis buffer (Thermo Fisher Scientific, Cat#: 89900) containing 1% Halt™ Protease Inhibitor Cocktail (Thermo Fisher Scientific Inc., Cat#: 78430) at days 0, 0.5, 1, 2, 3 and 7 after switching from SMC growth medium to NM or OM, for a total of six time points per condition per donor requiring four TMT 6-plex experiments. Cells were lysed and the protein was quantified using a Pierce™ BCA Protein Assay Kit (Thermo Fisher Scientific, Cat#: 23225). 50 μg protein was proteolyzed with LysC using the in-solution urea+ RapiGest (Waters) strategy.[1] Peptides were labeled with TMT 6-plex reagent (Thermo Fisher Scientific), combined and desalted using Oasis HLB 1 cc (10 mg) columns (Waters). The peptides were then fractionated into 24 fractions based on their isoelectric focusing point (pH range of 3 to 10) using the OFF-gel system (Agilent). Fractions were dried using a tabletop speed vacuum (Thermo Fisher Scientific), cleaned with Oasis columns, and resuspended in 40 μL of 5 % acetonitrile (Fisher Scientific), 0.5 % formic acid (Sigma-Aldrich) sample buffer for subsequent analysis by liquid chromatography/mass spectrometry (LC/MS).

SMCs label-free proteomics

SMCs incubated with *CROT* siRNA or scrambled siRNA were harvested from a single well of a 6-well plate, at 0, 6, 12 and 24 hours; and at 3, 7, 14 and 21 days after switching

from NM to OM (or NM for controls). Cells were washed with PBS then scraped from wells using 100 μL RIPA buffer and sonicated on ice to lyse cells. Proteolysis was performed using the iST kit (PreOmics GmbH) with 20 μg protein input with subsequent steps following the manufacturer's protocol. 1 μg of human recombinant CROT protein (OriGene Technologies, Inc., Cat#: TP307888) was digested also using the iST kit. Peptides were resuspended in 40 μL sample buffer. The recombinant CROT standard curve was first prepared in sample buffer for a final 0.1 to 100 pg CROT per injection, or spiked into a SMC peptide pool of the NM sample matrix for a final 1 to 100 pg CROT per injection.

Mass spectrometry

TMT peptide samples were analyzed with an LTQ-Orbitrap (Elite model) mass spectrometer fronted with a Nanospray FLEX ion source, and coupled to an Easy-nLC1000 HPLC pump (Thermo Fisher Scientific). Peptides were subjected to a dual column set-up: an Acclaim PepMap 100 C18 trap column, 75 μm X 20 mm; and an Acclaim PepMap RSLC C18 analytical column 75 μm X 250 mm (Thermo Fisher Scientific). An analytical gradient was run at 350 nL/min from 10 to 30 % solvent B (acetonitrile/0.1 % formic acid) for 120 minutes, followed by ten minutes of a 'jigsaw wash', alternating between 5 and 95 % solvent B. Solvent A was 0.1 % formic acid. All reagents were mass spectrometry-grade. The instrument was set to 120 K resolution, and the top 20 precursor ions (within a scan range of 380-2000 *m/z*) were subjected to higher energy collision induced dissociation (HCD, normalized collision energy 40%, isolation width 3 m/z, dynamic exclusion enabled, starting m/z fixed at 120 m/z, and resolution set to 30 K) for peptide sequencing (MS/MS).

For label-free analysis, peptides from silencing experiments were analyzed twice by global proteomics and targeted CROT proteomics, using an Orbitrap Fusion Lumos Tribrid mass spectrometer (Thermo Fisher Scientific) fronted with an Easy-Spray ion source, and coupled to an Easy-nLC1000 HPLC pump (Thermo Fisher Scientific). Peptides were separated using a dual column set-up: an Acclaim PepMap 100 C18 trap column, 75 μm X 20 mm; and an EASY-Spray HPLC heated (45 ^{o}C) column, 75 μm X 250 mm (Thermo Fisher Scientific). The gradient flow rate was 300 nL/min from 5 to 21% solvent B (acetonitrile/0.1% formic acid) for 75 minutes, 21 to 30 % solvent B for 15 minutes, followed by the jigsaw wash. The instrument was set to 120 K resolution, and the top N precursor ions in a 3 second cycle time (within a scan range of 375-1500 m/z; isolation window, 1.6 m/z; ion trap scan rate, normal) were subjected to collision induced dissociation (collision energy 30%) for peptide sequencing (or MS/MS). Dynamic exclusion was enabled (60 seconds). For CROT targeted mass spectrometry using parallel reaction monitoring, CROT peptides (VLNDINQAK, a.a. 376-384; FQSGIGEK, a.a.58-65) and ACTR2 peptides (DLmVGDEASELR, a.a. 54-65, M3 oxidized) were measured. The analytical gradient was run at 300 nL/min from 5 to 21% Solvent B for 20 minutes, 21 to 35% Solvent B for five minutes, followed by the jigsaw wash. The mass spectrometer was operated in the targeted acquisition mode. Precursor m/z values were 507.7824 for VLNDINQAK (charge, 2; time window, 11.0-14.5 min), 433.2246 for FQSGIGEK (charge, 2; time window, 9.0-13.0 min), and 675.8144 for DLmVGDEASELR (charge, 2; time window, 20.0-22.5 min) using an isolation window of 1.2 m/z. The MS/MS

spectra (collision energy, 30% HCD; scan range, 120-1200 m/z) were scanned at 240K resolution (Orbitrap).

Mass spectrometry data analysis

TMT data were queried against the human UniProt database (downloaded November, 2018) using the HT-SEQUEST search algorithm, via the Proteome Discoverer (PD) Package (version 2.1, Thermo Fisher Scientific) using a 10 ppm tolerance window in the MS1 search space, and a 0.02 Da fragment tolerance window for HCD. Methionine oxidation and 6-plex TMT labels were set as dynamic modifications, and carbamidomethylation of cysteine residues was set as a static modification. The peptide false discovery rate (FDR) was calculated using Percolator provided by PD: the FDR was determined based on the number of MS/MS spectral hits when searched against the reverse, decoy human database. Peptides were filtered based on a 1% false discovery rate. Peptides assigned to a given protein group, and not present in any other protein group, were considered as unique. Consequently, each protein group is represented by a single master protein (PD Grouping feature). Master proteins with two or more unique peptides were used for TMT reporter ratio quantification. *The label-free data for global proteomics* were queried against the human UniProt database (downloaded November, 2018) using the HT-SEQUEST search algorithm, via the Proteome Discoverer (PD) Package (version 2.2, Thermo Fisher Scientific). All donors and respective cell culture conditions (NM siSCR, OM siSCR and OM si*CROT*) were analyzed into a single consensus output file. Methionine oxidation and n-terminal acetylation were set as dynamic modifications, and carbamidomethylation of cysteine was set as a static modification. Peptides were filtered based on a 1% FDR based on the reverse database results. In order to quantify peptide precursors detected in the MS1 but not sequenced from sample to sample, we enabled the 'Feature Mapper' node. Chromatographic alignment was done with a maximum retention time (RT) shift of 10 minutes and a mass tolerance of 10 ppm. Feature linking and mapping settings were, RT tolerance minimum of 0 minutes, mass tolerance of 10 ppm and signal-to-noise minimum of five. Precursor peptide abundances were based on their chromatographic intensities and total peptide amount was used for normalization. Peptides assigned to a given protein group, and not present in any other protein group, were considered as unique. Consequently, each protein group is represented by a single master protein (PD Grouping feature). A unique and razor peptides per protein for quantification was used. Targeted CROT data were quantified with Skyline.[2] Peak area ratio (total area of CROT fragments/total area of ACTR2 fragments) was calculated using the following fragments: VLNDINQAK (CROT), *y7 m/z* 802.40 and *y8 m/z* 915.49; FQSGIGEK (CROT), *y6 m/z* 590.31 and *y3 m/z* 333.18; DLmVGDEASELR (ACTR2), *y8 m/z* 876.40, *y9 m/z* 975.47, and *b3 m/z* 376.15. A standard curve was constructed by plotting CROT concentration (y) vs nominal concentration of recombinant CROT (x).

Clustering analysis

High-dimensional clustering of the SMC siRNA protein datasets was done using k-means clustering provided by XINA (https://bioconductor.org/packages/XINA)[3], a software developed in our laboratory. XINA combines multiple quantitative proteomics data that

have a common underlying biology and experimental design, in this case, the SMC differentiation time course (0, 6, 12 and 24 hours; and 3, 7, 14 and 21 days for NM siSCR, OM siSCR and OM si*CROT*). Firstly, the protein abundance values for each donor dataset and respective cell culture conditions (NM siSCR, OM siSCR and OM si*CROT*) was median normalized[3]. All proteins that were detected at least one donor and one condition (3,925 proteins with two or more unique peptides) were used for XINA. In order to conduct the si*CROT* restoration analysis, we normalized each donor's OM siSCR and OM siCROT to the NM siSCR; and separated the time course analysis into an early phase (0hr, 6hr, 12hr and 24 hr) and a late phase (day3, day7, day14 and day21). Three proteomics datasets were therefore converted into two (per donor, per early and late phase) that were subsequently combined into a single dataset and analyzed by XINA (two conditions and three donors, total of six profiles per early and late phase). The resulting clusters therefore comprise mixtures of normalized OM siSCR and OM si*CROT* protein profiles that are distinguishable by XINA. K-means clustering was performed with multiple target clusters (eg. 6, 8, 10 and 20). A final number of 8 clusters was chosen since it captured similar cluster profiles across the three donor analyses.

Gene ontology enrichment of osteogenic induced SMCs

We used ConsensusPathDB[4] (database retrieved: March 4, 2020) and tested the set of 198 proteins showing an increase in OM in all donors and conditions for enrichment in pathways from KEGG, BioCarta and Reactome. We performed a hypergeometric test to determine the significance of enrichment and adjusted the resulting *p*-values for multiple testing using the Benjamini-Hochberg procedure to determine the false discovery rate (FDR). We have retained the complete list of all pathways with unadjusted $p \leq 0.05$ and considered pathways with FDR≤0.05 as significantly enriched.

Gene ontology enrichment of *CROT* siRNA restoration proteins

Thirty-eight proteins from a restoration list as well as 27 cardiovascular calcification-related GWAS proteins[5] were mapped to a Protein-Protein Interaction (PPI) network of 16,656 nodes and 243,592 edges compiled from 15 different sources.[6] 35 of the 38 proteins were found within the PPI network. 35 Mitochondrial proteins were selected among the first common neighbors of both the restoration and calcification modules. To elucidate biological processes associated with the different modules, we Gene Ontology (GO) annotations (http://www.geneontology.org/) and pathways (KEGG[7], Reactome[8], WikiPathways[9]) were used. In order to avoid noise and circularity analyses were restricted to proteins only mapped to Entrez gene IDs, excluding "NOT" qualifiers and considering only high confidence annotations associated with the evidence codes EXP, IDA, IMP, IGI, IEP, ISS, as listed below.

Experimental:

- Inferred from Experiment (EXP)
- Inferred from Direct Assay (IDA)
- Inferred from Mutant Phenotype (IMP)
- Inferred from Genetic Interaction (IGI)
- Inferred from Expression Pattern (IEP)

Computational:

- Inferred from Sequence or structural Similarity (ISS)

Analysis was further restricted to terms that are associated to 100 proteins or less to obtain more specific functions. GO enrichment tests were performed using ClueGO[10], a Cytoscape[11] add-on that facilitates the biological interpretation of large lists of genes and proteins by selecting representative GO terms and pathways from multiple ontologies and visualizes them into functionally organized networks. ClueGO was extended by CluePedia[12], allowing a detailed pathways analysis.

Total fatty acid assay

SMCs (n = 3 donors) were incubated with *CROT* siRNA or scrambled siRNA in NM for 7 days. Lipid was extracted and collected using isopropanol-hexane solution (isopropanol : hexane = 2 : 3). After drying up the solution, samples were dissolved using the assay buffer of Free Fatty Acid Assay Kit – Quantification (Abcam, Cat#: ab65341). Assay was performed using the manufacturer's protocol. Values were normalized by the abundance of protein measured by BCA assay.

Lipidomics analysis

SMCs (n = 4 donors) incubated with *CROT* siRNA or scrambled siRNA were harvested from two wells of a 6-well plate, at 3 and 7 days after switching from NM to OM (or NM for controls). Cells were washed with PBS then scraped from wells. Lipid analysis was performed at the UCSD Lipidomics Core.[13]

Fluorescence staining of mitochondria

SMCs incubated with *CROT* siRNA or scrambled siRNA were stained using MitoTracker™ Red CMXRos (Thermo Fisher Scientific Inc., Cat#: M7512) at 14 days after switching from NM to OM (or NM for controls). Cells were incubated with 100 nmol/L MitoTracker Red for 15 minutes at 37°C. Images were acquired using confocal microscopy (Nikon Instruments Inc.). Nuclear staining was performed with Hoechst 33342 Solution (BD Biosciences, Cat#: 561908). Mitochondrial aspect ratios were assessed using NIH ImageJ software.

Mitochondrial membrane potential assay

SMCs (n = 3 donors) were incubated with *CROT* siRNA or scrambled siRNA in 96-well plates, and the assay was performed at 14 days after switching from NM to OM (or NM for controls) by using TMRE Mitochondrial Membrane Potential Assay Kit (Abcam, Cat# ab113852).

Plasma lipid, glucose, AST and ALT assays

Mouse whole blood was drawn from inferior vena cava into heparinized microtubes and centrifuged at 10,000 times gravity for 10 minutes at 4°C. Plasma was collected and frozen at -80°C. Plasma levels of total cholesterol, triglycerides, free fatty acids and glucose were measured using commercial kits obtained from FUJIFILM Wako Diagnostics USA Corporation (cholesterol: Cat#: 439-17501, triglycerides: Cat#: 992-02892 and 998-02992, free fatty acids: Cat#: 999-34691, 991-34891, 995-34791 and 993-35191, glucose: Cat# 997-03001, AST:). Plasma AST and ALT levels were measured

using commercial kits obtained from MilliporeSigma (AST: Cat# MAK055-1KT, ALT: Cat# MAK052-1KT).

Histological analysis of mouse aorta

Tissue samples were frozen in OCT compound and serial sections were cut. Von Kossa silver stain was used to visualize inorganic phosphate calcium salts. Briefly, sections were incubated with 5% silver nitrate (American Master Tech Scientific) for 60 min under UV light, then washed with sodium thiosulfate. Nuclei were stained with nuclear fast red (American Master Tech Scientific). Then, we traced and quantified plaque and calcification area using NIS Elements 3.10 software (Nikon).

Micro-CT bone density scanning

Micro-CT scanning was performed at the Yale Core Center for Musculoskeletal Disorders microCT Facility. Briefly, femurs were soaked in 70% ethanol and stored at 4°C. Femurs were analyzed in 70% ethanol by cone beam microfocus x-ray computed tomography using a Scanco μCT-35 instrument (Scanco, Brutissellen, Switzerland). Images were acquired at 55 kVp, with an integration time of 500 milli-seconds and an isometric voxel size of 6 μm. Segmentation of bone from marrow and soft tissue was performed in conjunction with a constrained Gaussian filter (support=1; 3×3×3 voxel window; σ=0.8) to reduce noise, applying density thresholds of 250 and 420 for trabecular and cortical compartments of femur, respectively. Volumetric regions for trabecular analysis were selected within endosteal borders of distal femoral metaphysis to include secondary spongiosa located 1 mm from growth plate and extending 1 mm proximally, or from within cortical shell of the third lumbar vertebral body. Cortical morphometry was quantified and averaged volumetrically through 233 serial cross-sections (1.4 mm) centered on the diaphyseal midpoint between proximal and distal growth plates.

Supplemental figures, tables and legends

A

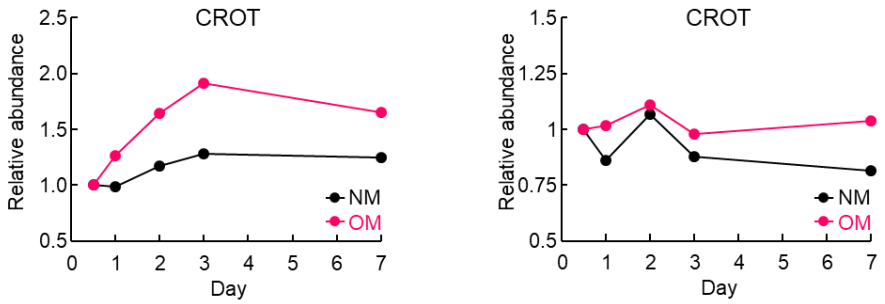

B **CROT (target) and ACTR2 (internal standard) fragments used for targeted proteomics**

Protein	Peptide	Retention time	Fragment
CROT	VLNDINQAK [376-384]	13.0 min	802.40 (y_7^+) 915.49 (y_8^+)
	FQSGIGEK [58-65]	11.9 min	590.31 (y_6^+) 333.18 (y_3^+)
ACTR2	DLmVGDEASELR [54-65] (M3 oxidized)	21.3 min	876.40 (y_8^+) 975.47 (y_9^+) 376.15 (b_3^+)

C

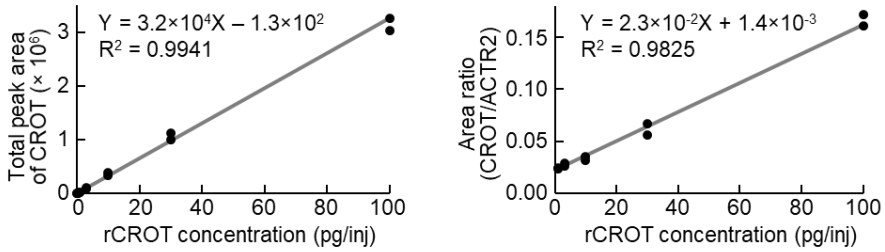

D

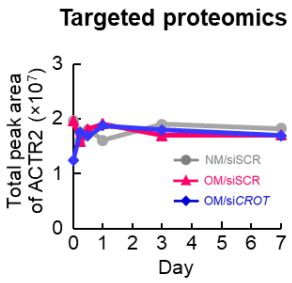

Supplemental Figure I. CROT abundance in TMT labeled proteomics data and CROT-targeted label-free proteomics. A, CROT abundance detected by TMT labeled proteomic analysis is shown. B, Fragments used for CROT-targeted proteomics are shown. C, Standard curves of CROT used in CROT-targeted proteomics are shown. Standard curves were made through measuring recombinant human CROT (rCROT). D, Time dependent changes of total peak area of ACTR2 in CROT-targeted proteomics are shown. ACTR2 was used as an internal control for CROT-targeted proteomics.

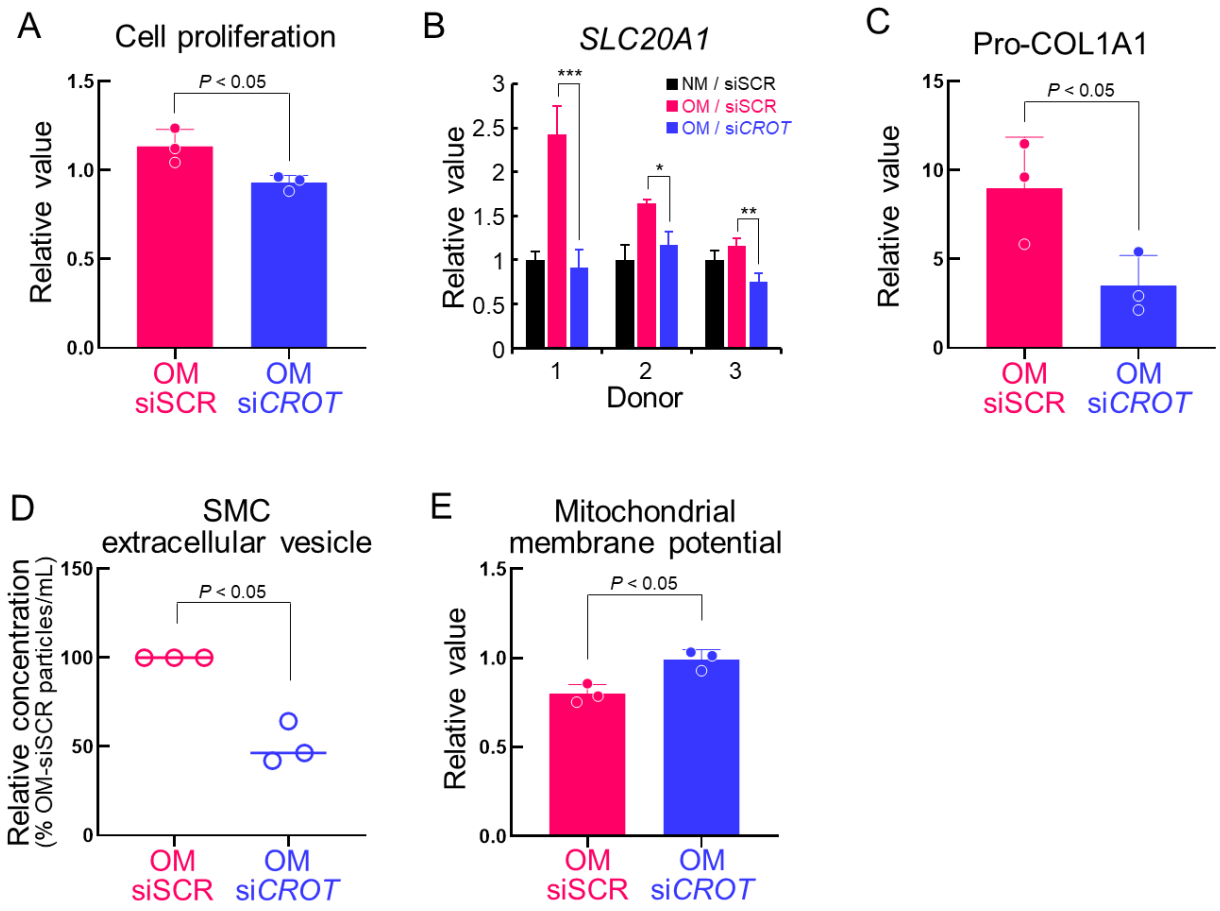

Supplemental Figure II. Effects of *CROT* siRNA on calcifying human vascular SMCs. A, Cell proliferation was measured using DNA intercalater at day 7. Values were normalized by NM/siSCR treated group; n = 3 donors, error bars are mean±SD, analyzed by Student's *t*-test. B, *SLC20A1* mRNA expression in human vascular SMCs was measured through real-time PCR using 3 donors. Error bars are mean±SD, analyzed by ANOVA with Tukey's multiple comparison test, ***P<0.001, **P<0.01, *P<0.05. C, Pro-collagen 1A1 in culture media was measured by ELISA. Day 5-7 media was used; n = 3 donors, error bars are mean±SD, analyzed by Student's t-test. D, Concentration of human SMC extracellular vesicle in culture media was measured using NanoSight. Media were collected at day 7. Values were normalized by OM/siSCR. Bars are mean, analyzed by Welch's *t*-test. E, Mitochondrial membrane potential was measured using TMRE reagent. Assay was performed at day 14; n = 3 donors, error bars are mean±SD, analyzed by Student's *t*-test.

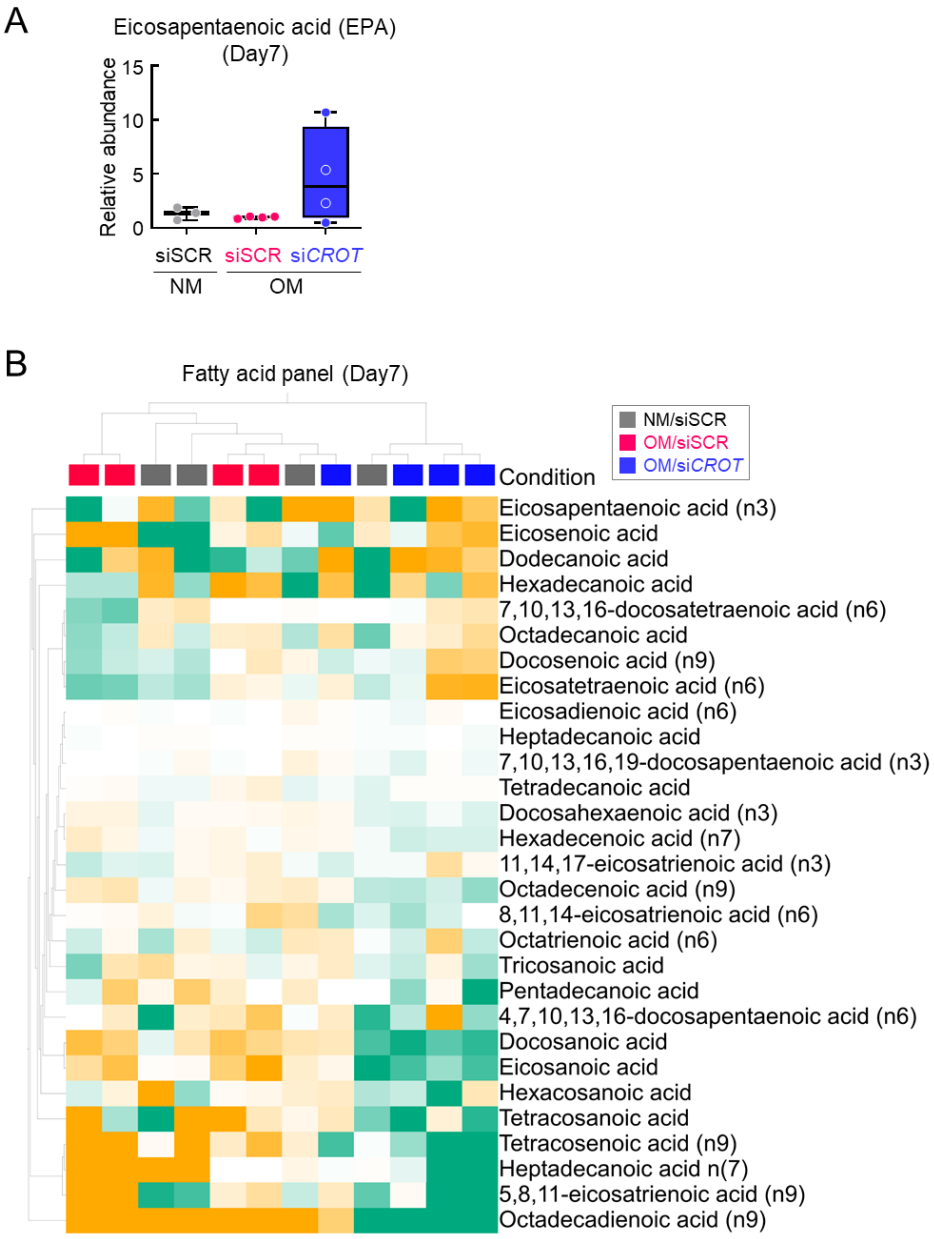

Supplemental Figure III. *CROT* silencing increased eicosapentaenoic acid (EPA) in SMCs. A, Relative abundance of EPA in SMCs treated with NM/siSCR, OM/siSCR, or OM/si*CROT* for 7 days was shown. Data was obtained through gas chromatography-mass spectrometry (GC-MS) and normalized by the abundance of total protein (4 donors, box-and-whiskers plots, Dunn's multiple comparison test). B, Heat map of fatty acid abundance obtained through GC-MS was shown (day 7). Each column represents each experimental condition (NM/siSCR: gray, OM/siSCR: magenta, OM/si*CROT*: blue) and donor (4 donors/condition). Each row represents each fatty acid. Color in heat map reflect abundance of fatty acid (high: yellow, low: green).

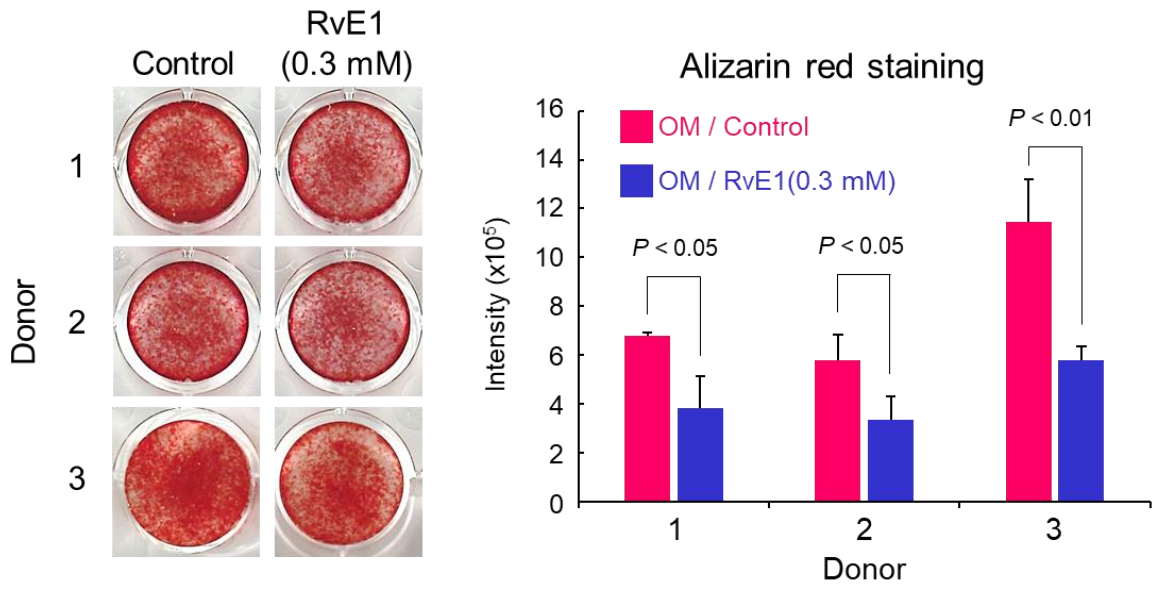

Supplemental Figure IV. RvE1 reduced calcium deposition in human SMCs. Human SMCs were treated with OM (control) or OM including 0.3 mM RvE1 and Alizarin red staining was performed at day 21 (n = 3 donors). Representative images are shown at left panel. Alizarin red intensity was quantified using Image J software (right panel); 3 technical replicates per donor, error bars are mean±SD, analyzed by Student's *t*-test.

A

Name	Transcript ID	bp	Protein	Biotype	CCDS	UniProt	Flags
Crot-201	ENSMUST 00000003720.4	2996	612aa	Protein coding	CCDS 19087	Q9DC50	TSL:1 GENCODE basic APPRIS P1
Crot-202	ENSMUST 00000146115.1	1006	No protein	Processed transcript	-	-	TSL:5
Crot-203	ENSMUST 00000157024.1	2746	No protein	Retained intron	-	-	TSL:1

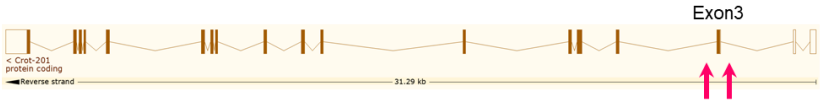

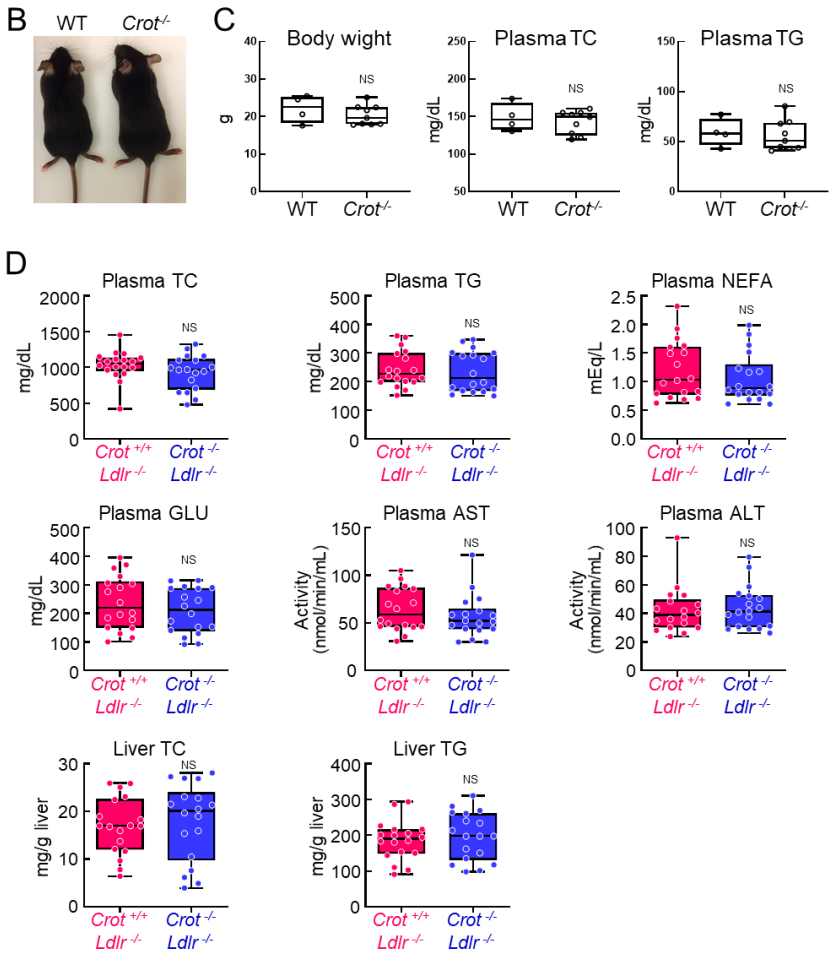

Supplemental Figure V. Blood biochemistry and liver lipids of *Crot* and *Ldlr* deficient mice. A, Table of Crot transcript variants is shown. *Crot*$^{-/-}$ mice were generated by removing *Crot* exon 3 that includes the start codon of *Crot* in C57BL/6J mice using CRISPR-Cas9 system (The Jackson Laboratory). B, Gross image of 10-week-old wildtype and Crot-/- mouse. C, Blood biochemistry of Crot-/- mice (10-week-old, 4-9 mice/group, box-and-whiskers plots, Student's *t*-test, ns: not significant) D, Blood biochemistry and liver lipids of *Crot*$^{+/+}$*Ldlr*$^{-/-}$ and *Crot*$^{-/-}$*Ldlr*$^{-/-}$ mice are shown (18 mice/group, box-and-whiskers plots, Student's t-test, ns: not significant).

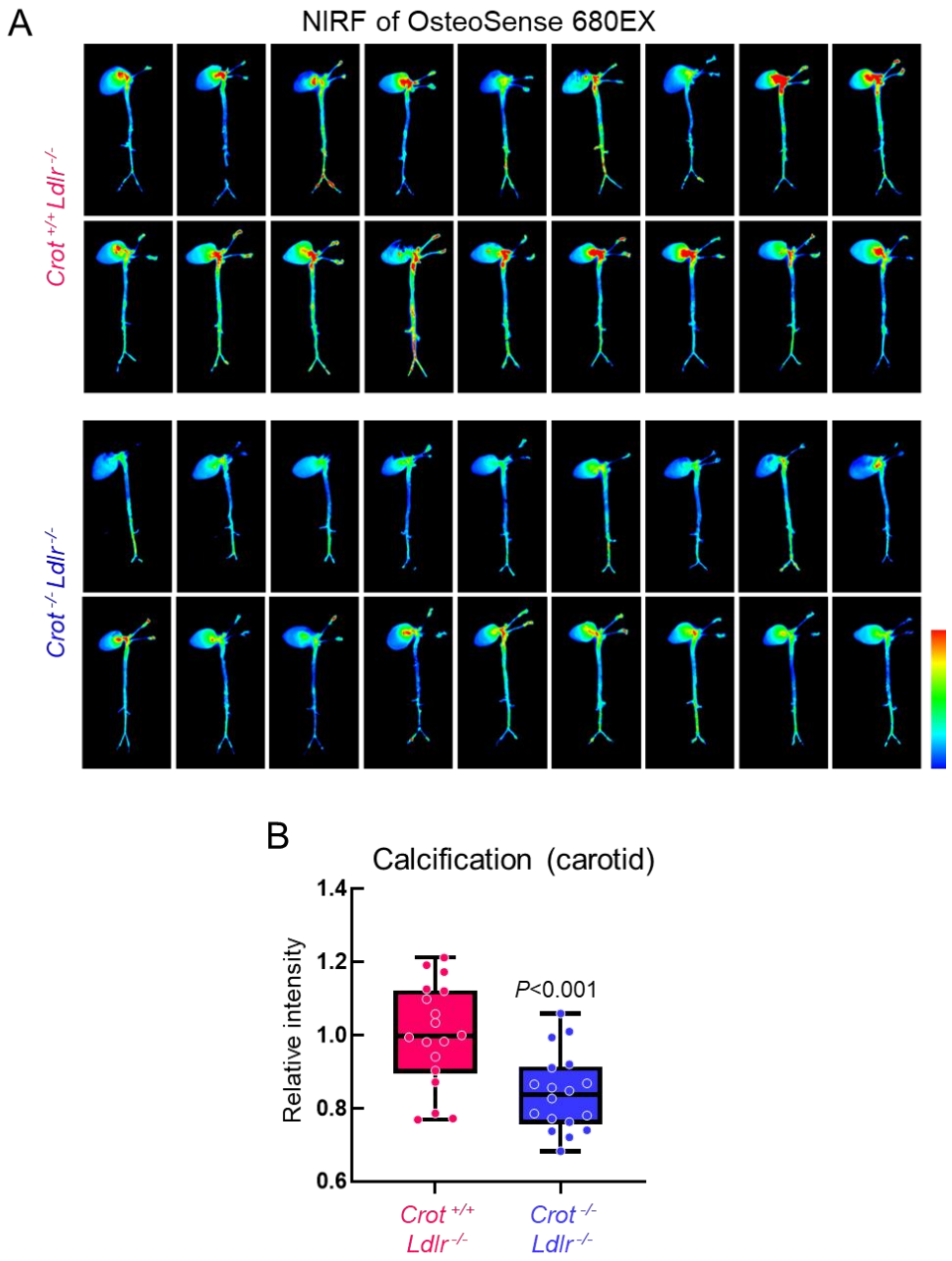

Supplemental Figure VI. Vascular calcification was reduced by *Crot* deficiency in *Ldlr*$^{-/-}$ mice. A, Near-infrared fluorescence (NIRF) of OsteoSense 680EX on heart/aorta/carotid artery was taken *ex vivo*. OsteoSense 680EX heat map images of all mice are shown (high: red, low: blue). *Crot*$^{+/+}$*Ldlr*$^{-/-}$ and *Crot*$^{-/-}$*Ldlr*$^{-/-}$ mice were fed HFHC diet for 15 weeks. 18 mice/group. B, Quantification result of OsteoSense 680EX intensity of carotid artery. 18 mice/group, box-and-whiskers plots, analyzed by Student's *t*-test.

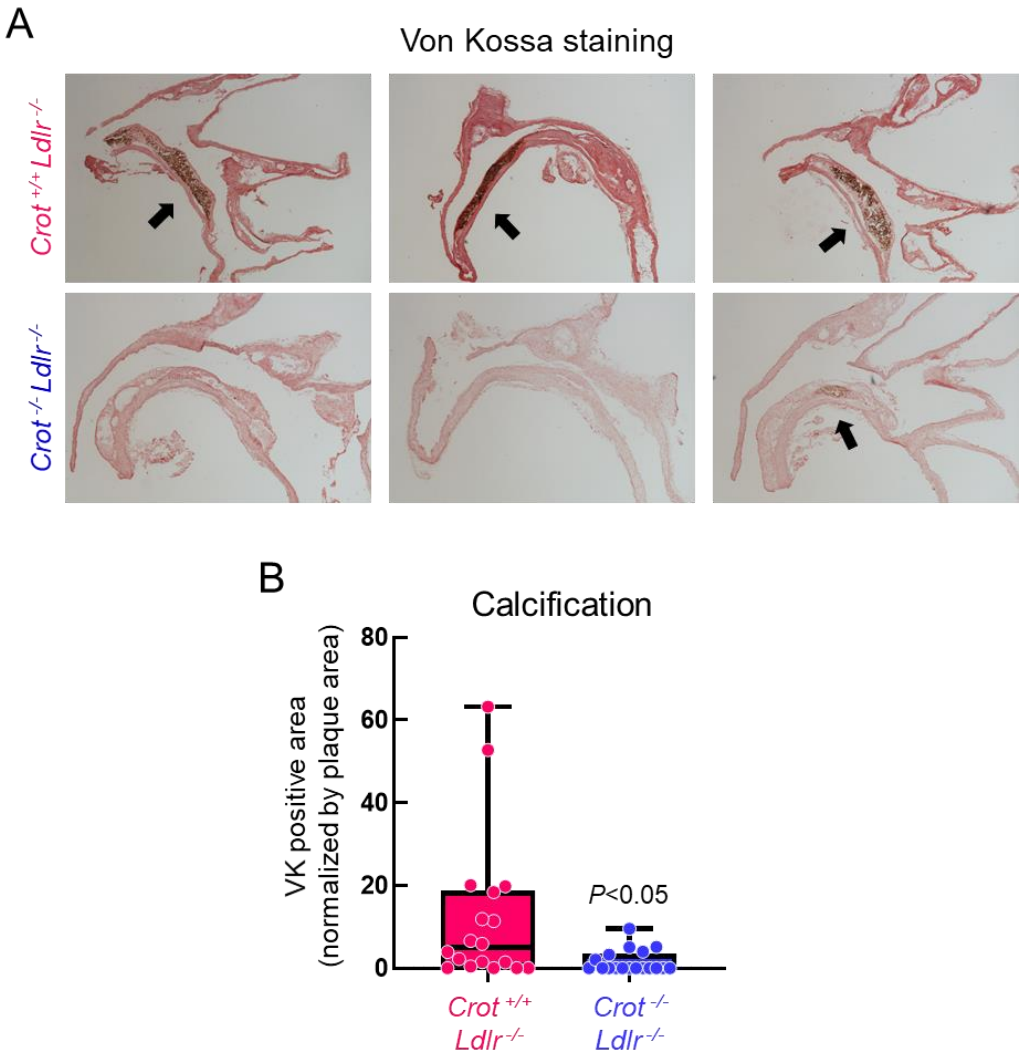

Supplemental Figure VII. Vascular calcification was reduced by *Crot* deficiency in *Ldlr*$^{-/-}$ mice. A, Additional representative images of von Kossa staining on aortic arch region are shown. *Crot*$^{+/+}$*Ldlr*$^{-/-}$ and *Crot*$^{-/-}$*Ldlr*$^{-/-}$ mice were fed HFHC diet for 15 weeks. Calcified region was stained brown (arrow). B, calcification area (von Kossa staining positive area) was quantified and normalized by the area of plaque. 18 mice/group, box-and-whiskers plots, analyzed by Student's *t*-test.

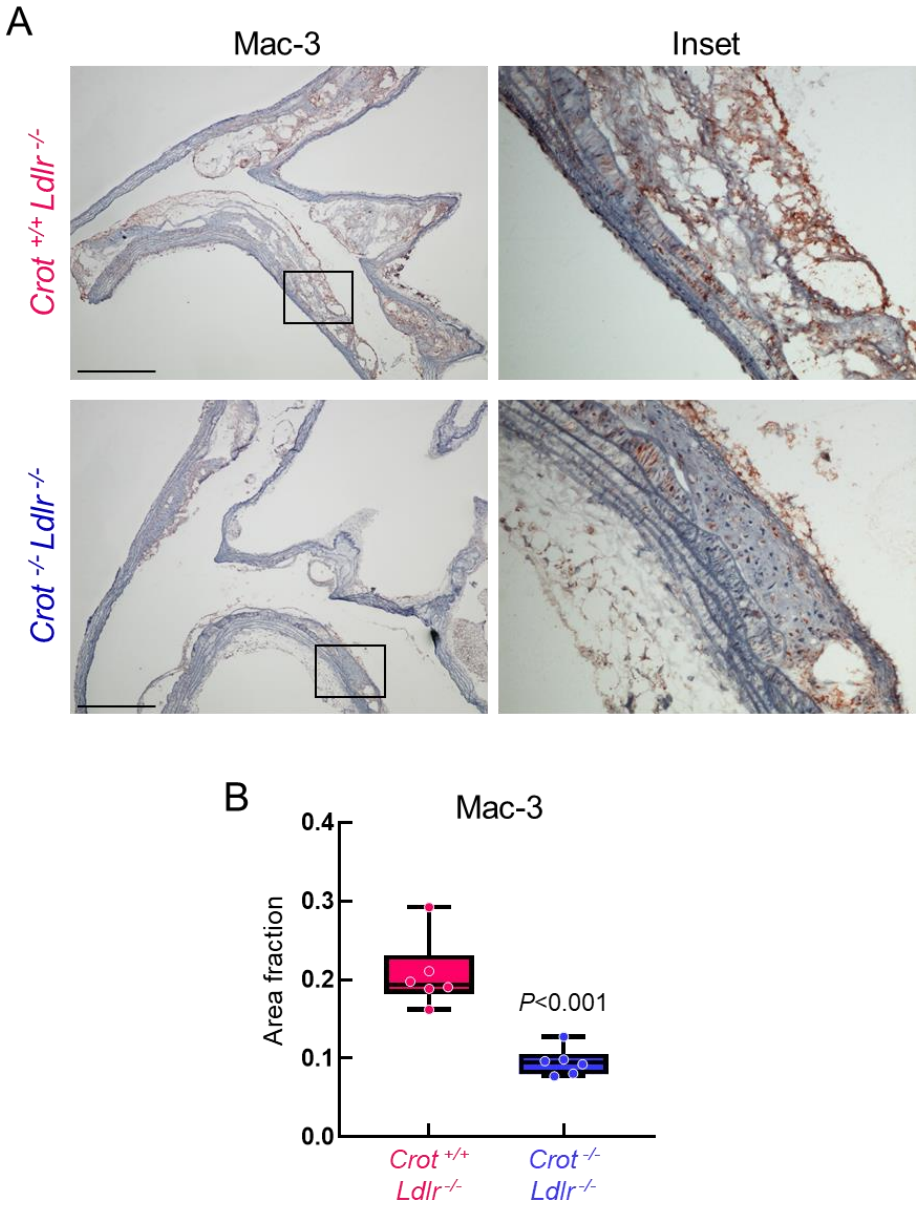

Supplemental Figure VIII. Macrophage accumulation was reduced by *Crot* deficiency in *Ldlr*$^{-/-}$ mice. A, Representative images of Mac-3 immunohistochemistry on aortic arch region are shown. Positive region stained brown color. Scale bars represent 2 mm. B, Mac-3 positive area was quantified. 6 mice/group, box-and-whiskers plots, analyzed by Student's *t*-test.

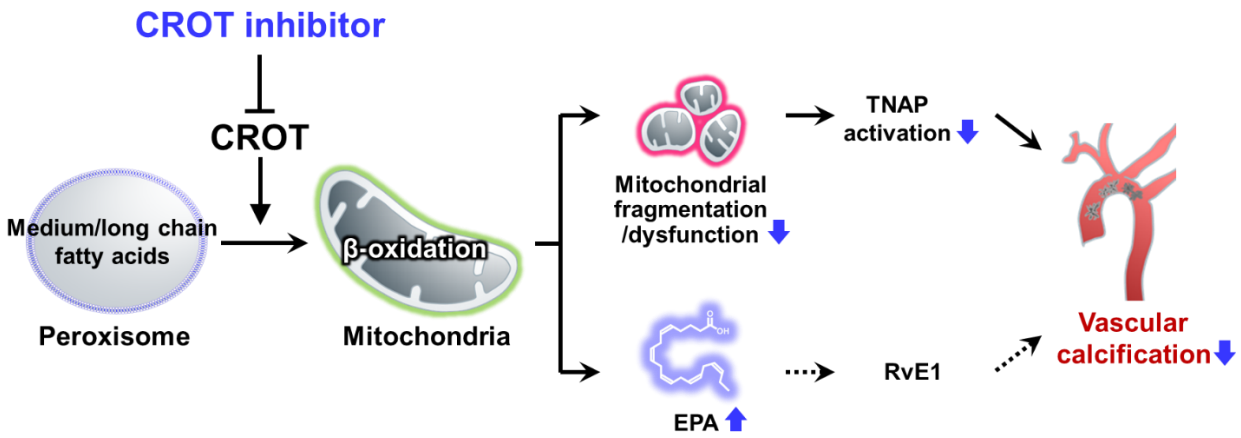

Supplemental Figure IX. Working model. CROT likely induced vascular calcification by promoting select fatty acid metabolism and mitochondrial dysfunction. CROT metabolizes select fatty acids in peroxisomes, allowing medium chain fatty acids to traffic from peroxisomes to mitochondria where they are further metabolized by β-oxidation. Increased CROT activity likely increased fatty acid trafficking to mitochondria inducing mitochondrial dysfunction and fragmentation. Additionally, increased CROT activity may reduce EPA by increasing select fatty acid metabolism. Dysfunctional mitochondria promote TNAP activity, which induced vascular calcification. CROT inhibition, reduced select fatty acid metabolism that attenuated mitochondria dysfunction and increased EPA, leading to reduced TNAP activity and vascular calcification.

Supplemental Table I.

Mitochondrial cluster	ACAT1	ATP5A1	ATP5B	C1QBP	CLPP
	COQ8A	ECHS1	FASTKD3	FECH	FXN
	HSPA9	HSPD1	IDH3G	MRPL12	MRPL55
	MRPL58	MRPS2	MRPS7	NDUFA10	NDUFA9
	NDUFB11	NDUFB5	NDUFS1	NDUFV2	PITRM1
	PRDX5	PTCD3	SCO2	SDHA	SDHAF2
	SIRT4	SIRT5	SSBP1	STOML2	TRAP1
Restoration cluster	ATP5F1D	CAPZA1	CAPZB	CLTA	CRYZ
	F2	FCGRT	GAK	GMFB	GSN
	HSPE1	IDH3B	KTN1	LRP1	MKRN2
	MYO9B	NDUFB3	NT5DC1	NUDT5	PEAK1
	PLCD1	PPP2R1A	PSMD5	RHOG	SDHB
	SH3GLB1	SNRPC	STOM	SUCLG2	SYNCRIP
	TCEAL3	TCIRG1	TMED5	TPM3	UBE2I
	ATP5F1D	CAPZA1	CAPZB	CLTA	CRYZ
Calcification cluster	ABCA4	ACTA2	ADAMTS7	ADAMTS9	ATP2B1
	CACNA1C	CDKN2A	CDKN2B	COL4A1	COL4A2
	GLIS1	KCNJ2	LPA	MRAS	NOTCH1
	OPCML	PALMD	PHACTR1	PRKG2	RUNX2
	SORT1	TBC1D4	TCF7L2	TGFBR1	TGFBR2
	TNFRSF8	WWOX			

Supplemental Table I. Proteins used for functionally grouped network of enriched pathways/GO and BP terms for mitochondrial proteins (green), si*CROT* restoration proteins (blue) and calcification-related proteins (red) are shown (See Figure 3C, 3D and Supplemental figure II-IV).

	Cortical		Trabecular	
	Crot $^{+/+}$ *Ldlr* $^{-/-}$	*Crot* $^{-/-}$ *Ldlr* $^{-/-}$	*Crot* $^{+/+}$ *Ldlr* $^{-/-}$	*Crot* $^{-/-}$ *Ldlr* $^{-/-}$
TV	1.282 (0.122)	1.302 (0.074)	3.344 (0.052)	3.411 (0.212)
BV	1.146 (0.116)	1.152 (0.070)	0.543 (0.118)	0.510 (0.153)
BV/TV	0.893 (0.011)	0.885 (0.016)	0.163 (0.037)	0.149 (0.042)
Conn-Dens.	-	-	177.792 (12.264)	197.347 (6.383)
SMI	-	-	1.300 (0.369)	1.575 (0.239)
Tb.N	-	-	4.211 (0.060)	4.238 (0.098)
Tb.Th	-	-	0.048 (0.006)	0.046 (0.004)
Tb.Sp	-	-	0.231 (0.003)	0.231 (0.005)
Ct.Th	0.170 (0.015)	0.169 (0.006)	-	-
Apparent Density (of TV)	982.380 (28.191)	961.445 (36.978)	155.676 (31.819)	137.614 (23.102)
Bone Tissue Density (of BV) [mg HA/ccm]	1072.338 (31.817)	1054.512 (35.534)	810.911 (28.753)	808.182 (14.939)
BS	14.683 (0.602)	14.728 (0.806)	30.219 (2.873)	30.305 (5.729)
BS/BV	12.887 (1.166)	12.778 (0.674)	57.238 (9.642)	61.231 (7.158)
DA	-	-	1.713 (0.139)	1.548 (0.052)
endosteal radius	0.857 (0.159)	0.839 (0.044)	-	-
periosteal radius	1.026 (0.148)	1.009 (0.040)	-	-
endosteal circumference	5.380 (1.000)	5.271 (0.275)	-	-
periosteal circumference	6.445 (0.932)	6.335 (0.253)	-	-
pMOI	0.552 (0.068)	0.547 (0.062)	-	-

Supplemental Table II. Micro computed tomography (micro-CT) data of *Crot*$^{+/+}$*Ldlr*$^{-/-}$ and *Crot*$^{-/-}$*Ldlr*$^{-/-}$ mice femurs are shown. Mice were fed HFHC diet for 15 weeks. (5 mice/each group, mean values and SD in parentheses). TV: total volume, BV: bone volume, Conn-Dens.: Connectivity density, SMI: structure model index, Tb.N: trabecular number, Tb.Th: trabecular thickness, Tb.Sp: trabecular separation, Ct.Th: cortical thickness, BS: bone surface, DA: Degree of anisotropy.

References

1. Itou T, Maldonado N, Yamada I, Goettsch C, Matsumoto J, Aikawa M, Singh SA, Aikawa E. Cystathionine γ-lyase Accelerates Osteoclast Differentiation: Identification of a Novel Regulator of Osteoclastogenesis by Proteomic Analysis. *Arterioscler Thromb Vasc Biol*. 2014;34:626-634. doi: 10.1161/ATVBAHA.113.302576.
2. MacLean B, Tomazela DM, Shulman N, Chambers M, Finney GL, Frewen B, Kern R, Tabb DL, Liebler DC, MacCoss MJ. Skyline: An Open Source Document Editor for Creating and Analyzing Targeted Proteomics Experiments. *Bioinformatics*. 2010;26:966-968. doi: 10.1093/bioinformatics/btq054.
3. Lee LH, Halu A, Morgan S, Iwata H, Aikawa M, Singh SA. XINA: A Workflow for the Integration of Multiplexed Proteomics Kinetics Data With Network Analysis. *J Proteome Res*. 2019;18:775-781. doi: 10.1021/acs.jproteome.8b00615.
4. Kamburov A, Pentchev K, Galicka H, Wierling C, Lehrach H, Herwig R. ConsensusPathDB: Toward a More Complete Picture of Cell Biology. *Nucleic Acids Res*. 2011;39(Database issue):D712-7. doi: 10.1093/nar/gkq1156.
5. Rogers MA, Aikawa E. Cardiovascular calcification: artificial intelligence and big data accelerate mechanistic discovery. *Nat Rev Cardiol*. 2019;16:261-274. doi: 10.1038/s41569-018-0123-8.
6. Cheng F, Kovács IA, Barabási AL. Network-based Prediction of Drug Combinations. *Nat Commun*. 2019;10:1197. doi: 10.1038/s41467-019-09186-x.
7. Kanehisa M, Goto S. KEGG: Kyoto Encyclopedia of Genes and Genomes. *Nucleic Acids Res*. 2000;28:27-30. doi: 10.1093/nar/28.1.27.
8. Jassal B, Matthews L, Viteri G, Gong C, Lorente P, Fabregat A, Sidiropoulos K, Cook J, Gillespie M, Haw R, Loney F, May B, Milacic M, Rothfels K, Sevilla C, Shamovsky V, Shorser S, Varusai T, Weiser J, Wu G, Stein L, Hermjakob H, D'Eustachio P. The Reactome Pathway Knowledgebase. *Nucleic Acids Res*. 2020;48:D498-D503. doi: 10.1093/nar/gkz1031.
9. Slenter DN, Kutmon M, Hanspers K, Riutta A, Windsor J, Nunes N, Mélius J, Cirillo E, Coort SL, Digles D, Ehrhart F, Giesbertz P, Kalafati M, Martens M, Miller R, Nishida K, Rieswijk L, Waagmeester A, Eijssen LMT, Evelo CT, Pico AR, Willighagen EL. WikiPathways: A Multifaceted Pathway Database Bridging Metabolomics to Other Omics Research. *Nucleic Acids Res*. 2018;46:D661-D667. doi: 10.1093/nar/gkx1064..
10. Bindea G, Mlecnik B, Hackl H, Charoentong P, Tosolini M, Kirilovsky A, Fridman WH, Pages F, Trajanoski Z and Galon J. ClueGO: A Cytoscape Plug-In to Decipher Functionally Grouped Gene Ontology and Pathway Annotation Networks. *Bioinformatics*. 2009;25:1091-1093. doi: 10.1093/bioinformatics/btp101.
11. Shannon P, Markiel A, Ozier O, Baliga NS, Wang JT, Ramage D, Amin N, Schwikowski B, Ideker T. Cytoscape: A Software Environment for Integrated Models of Biomolecular Interaction Networks. *Genome Res*. 2003;13:2498-504. doi: 10.1101/gr.1239303.

12. Bindea G, Galon J, Mlecnik B. CluePedia Cytoscape Plugin: Pathway Insights Using Integrated Experimental and in Silico Data. *Bioinformatics*. 2013;29:661-663. doi: 10.1093/bioinformatics/btt019.
13. Quehenberger O, Armando AM, Brown AH, Milne SB, Myers DS, Merrill AH, Bandyopadhyay S, Jones KN, Kelly S, Shaner RL, Sullards CM, Wang E, Murphy RC, Barkley RM, Leiker TJ, Raetz CRH, Guan Z, Laird GM, Six DA, Russell DW, McDonald JG, Subramaniam S, Fahy E, Dennis EA. Lipidomics Reveals a Remarkable Diversity of Lipids in Human Plasma. *J Lipid Res*. 2010;51:3299-3305. doi: 10.1194/jlr.M009449.

Major Resources Table

Animals (*in vivo* studies)

Species	Vendor or Source	Background Strain	Sex
Mouse: *Crot*$^{+/+}$*Ldlr*$^{-/-}$	The Jackson Laboratory	C57BL/6J	M
Mouse: *Crot*$^{-/-}$*Ldlr*$^{-/-}$	The Jackson Laboratory	C57BL/6J	M

Genetically Modified Animals

	Species	Vendor or Source	Background Strain	Other Information
Parent - Male	Mouse	The Jackson Laboratory	C57BL/6J	*Crot* deficient, F0-F1
Parent - Female	Mouse	The Jackson Laboratory	C57BL/6J	*Crot* deficient, F0-F1
Parent - Male	Mouse	The Jackson Laboratory	B6.129S7-*Ldlr*^{tm1Her}/J	For crossbreeding with *Crot* deficient mice
Parent - Female	Mouse	The Jackson Laboratory	B6.129S7-*Ldlr*^{tm1Her}/J	For crossbreeding with *Crot* deficient mice

Antibodies

Target antigen	Vendor or Source	Catalog #	Working concentration
CROT	Abcam plc.	ab103448	20 μ g/mL
αSMA	Enzo Life Sciences, Inc.	ENZ-C34931	1:50
Mac-3	BD Pharmingen™	550292	1.6 µg/mL
Rabbit IgG	Vector Laboratories.	BA-1000	1:500
Rabbit IgG	Thermo Fisher Scientific Inc.	A-11070	1:1000
Mouse IgG	Thermo Fisher Scientific Inc.	A-21203	1:500

Cultured cell line

Name	Vendor	Catalog #
293A Cell Line	Thermo Fisher Scientific Inc.	R70507

Cultured primary cells

Name	Vendor	Sex	Age	Race	Catalog #
Human coronary artery smooth muscle cells	PromoCells	F	38	Caucasian	C-12511
		F	63	Asian	
		M	55	Caucasian	
		M	58	Caucasian	

Primers for real-time PCR

Gene	Species	Product name	Vendor	Persistent ID
CROT	Human	TaqMan® Gene Expression Assays (FAM)	Thermo Fisher Scientific Inc.	Hs00221733_m1
GAPDH	Human	TaqMan® Gene Expression Assays (FAM)	Thermo Fisher Scientific Inc.	Hs02758991_g1

Primers for generating H327A-CROT

Name	Species	Sequence	Vendor
H327A-CROT Forward	Human	5'-GTGATGCTGCTCCTTT TGATGCAATGATTATGG-3'	Integrated DNA Technologies, Inc.
H327A-CROT Reverse	Human	5'-AGGAGCAGCATCACAA TTACAGCCAAATACTCC-3'	Integrated DNA Technologies, Inc.

Primers for genotyping

Gene	Species	Sequence	Vendor
Crot (wild/mutant) Forward	Mouse	5'-AATATCCCAT GCTCCACACC-3'	Integrated DNA Technologies, Inc.
Crot (wild/mutant) Reverse	Mouse	5'-GAGAATGTGA GGGAAATTTGGA-3'	Integrated DNA Technologies, Inc.
Ldlr (wild) Forward	Mouse	5'-GAAGGTCCGCTC TCTGACCCTGTTAC-3'	Integrated DNA Technologies, Inc.
Ldlr (wild) Reverse	Mouse	5'-GTTGTATGATGCC GACAGTGAACGC-3'	Integrated DNA Technologies, Inc.
Ldlr (mutant) Forward	Mouse	5'-TTACTCCTGGGCGA AGATGCTAGAAGG-3'	Integrated DNA Technologies, Inc.
Ldlr (mutant) Reverse	Mouse	5'-TGGACACTTGCTTC TGGAAGTCCTCATAC-3'	Integrated DNA Technologies, Inc.

sgRNA for generating *Crot*$^{-/-}$ mice

Target	Sequence	Vendor
Intron 2 of *Crot*	5'-ACACCACACTACCTGGGGTT-3'	The Jackson Laboratory
	5'-AACACCACACTACCTGGGGT-3'	
	5'-CTCTAACACCACACTACCTG-3'	
	5'-CCACCCAACCCCAGGTAGTG-3'	
Intron 3 of *Crot*	5'-CCTTGTACTAAGTCCACGGA-3'	
	5'-TCCTTGTACTAAGTCCACGG-3'	
	5'-ATCTCCTTGTACTAAGTCCA-3'	

	5’-CCCTCCGTGGACTTAGTACA-3’	

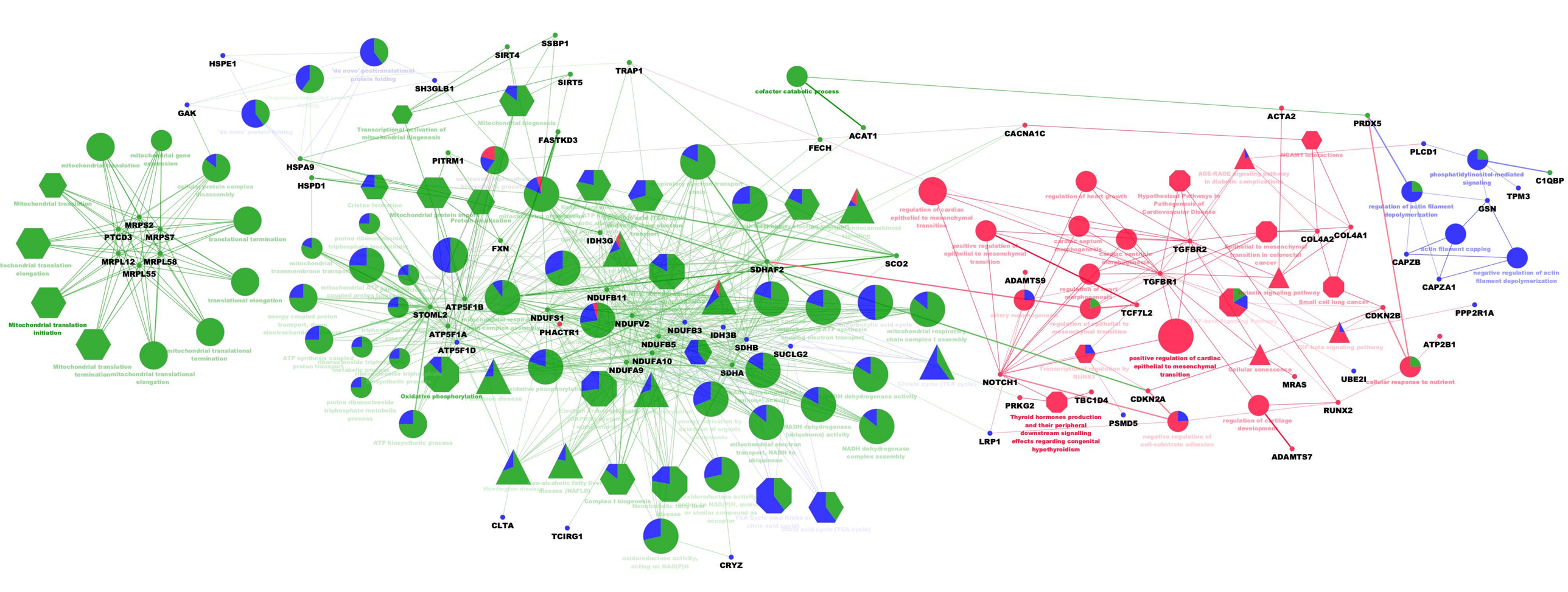
HSPE1
'de novo' posttranslational protein folding
SSBP1
SIRT4
SH3GLB1
SIRT5
TRAP1
GAK
'de novo' protein folding
Transcriptional activation of mitochondrial biogenesis
Mitochondrial biogenesis
FASTKD3
PITRM1
HSPA9
HSPD1
Cristae formation
Mitochondrial protein import
Protein localization
FXN
IDH3G
SCO2
SDHAF2
NDUFB11
NDUFS1
NDUFV2
PHACTR1
NDUFB3
IDH3B
NDUFB5
SDHB
SUCLG2
NDUFA10
SDHA
NDUFA9
ATP5F1B
STOML2
ATP5F1A
ATP5F1D
Oxidative phosphorylation
ATP biosynthetic process
Huntington disease
Non-alcoholic fatty liver disease (NAFLD)
Complex I biogenesis
Nonalcoholic fatty liver disease
oxidoreductase activity, acting on NAD(P)H
TCA Cycle and Krebs or citric acid cycle
citric acid cycle (TCA cycle)
mitochondrial electron transport, NADH to ubiquinone
NADH dehydrogenase (ubiquinone) activity
NADH dehydrogenase complex assembly
Citrate cycle (TCA cycle)
mitochondrial respiratory chain complex I assembly
CLTA
TCIRG1
CRYZ
cofactor catabolic process
ACAT1
FECH
mitochondrial translation
mitochondrial gene expression
cellular protein complex disassembly
Mitochondrial translation
MRPS2
PTCD3
MRPS7
translational termination
MRPL12
MRPL58
MRPL55
translational elongation
Mitochondrial translation elongation
Mitochondrial translation initiation
mitochondrial translational termination
Mitochondrial translation termination
mitochondrial translational elongation
CACNA1C
regulation of cardiac epithelial to mesenchymal transition
positive regulation of epithelial to mesenchymal transition
ADAMTS9
TGFBR1
TCF7L2
regulation of heart morphogenesis
artery morphogenesis
regulation of epithelial to mesenchymal transition
NOTCH1
PRKG2
TBC1D4
Thyroid hormones production and their peripheral downstream signalling effects regarding congenital hypothyroidism
LRP1
PSMD5
CDKN2A
negative regulation of cell-substrate adhesion
positive regulation of cardiac epithelial to mesenchymal transition
Transcriptional regulation by RUNX3
ACTA2
PRDX5
NCAM1 interactions
regulation of heart growth
Hypothesized Pathways in Pathogenesis of Cardiovascular Disease
AGE-RAGE signaling pathway in diabetic complications
cardiac septum morphogenesis
Cardiac ventricle morphogenesis
TGFBR2
COL4A2
COL4A1
Epithelial to mesenchymal transition in colorectal cancer
Relaxin signaling pathway
Small cell lung cancer
CDKN2B
PPP2R1A
ATP2B1
TGF-beta signaling pathway
Cellular senescence
MRAS
UBE2I
Cellular response to nutrient
RUNX2
regulation of cartilage development
ADAMTS7
PLCD1
phosphatidylinositol-mediated signaling
C1QBP
TPM3
regulation of actin filament depolymerization
GSN
actin filament capping
CAPZB
CAPZA1
negative regulation of actin filament depolymerization